Competition Between Ponderomotive and Thermal Forces in Short-Scale-Length Laser-Plasmas

X. Liu and D. Umstadter

Center for Ultrafast Optical Science, University of Michigan, Ann Arbor, MI 48109-2099

Abstract

The interactions of intense 1-ps and 400-fs laser pulses with a solid target are studied with time-integrated and time-resolved measurements. The latter are accomplished by means of a pump and probe experiment, in which the motion of the critical surface is measured with 250-fs temporal resolution. It is found that when the average electron quiver energy ($mv_{os}^2/2$) becomes comparable to the electron thermal energy (kT_e), the ponderomotive force of the high-intensity laser significantly reduces the thermal expansion of a laser-plasma. This study is performed in an interesting regime not easily accessible with longer pulse lasers, in which the electron density scale length during the laser pulse was much less than the laser wavelength.

When an intense laser interacts with a solid target, a thermal pressure gradient, inversely proportional to the density scale length (d), causes a rapid expansion of the plasma into the vacuum. This force is opposed by the pressure gradient of the laser light, known as the ponderomotive force. When the laser light is reflected from the plasma, twice its momentum is imparted to the plasma at the reflection point, near the critical surface, z_c, the point along the density profile where the incident laser frequency, ω_0, equals the plasma frequency, ω_p. Reported in this Letter are results indicating that the ponderomotive force may significantly impede the thermal expansion of even an extremely short density scale length plasma, one in which $d << \lambda$, the laser wavelength. As such they have important implications for the deposition of laser energy at solid density with applications to compact coherent or incoherent x-ray sources [1]–[3]. This limit is studied experimentally by using a short-pulse laser (400 fs)—since in this case relatively little expansion occurs before the peak of the pulse—and numerically by solving the wave equation. The effect was first studied in the long-pulse regime ($\lambda \leq d$), experimentally by use of interferometry [4], and analytically by use of the WKB approximation [5].

In order to determine the velocity at which the critical surface expands, $v_{\rm exp}$, which is in a direction normal to the surface of a planar target, the Doppler-shift ($\Delta\lambda/\lambda = -2(v_{\rm exp}/c)\cos\theta$) of light reflected from z_c was measured, where θ is the angle of incidence. A simple model that assumes the motion is governed only by thermal pressure (*i.e.*, free expansion) has previously been used to determine the plasma temperature from

measurements of the Doppler shift of the pump light [6]. However, at higher laser intensities, such as those used in our experiment, this procedure is expected to yield misleading results [7][8]. In addition, the Doppler shift of the reflected pump light yields only time-integrated information about the motion of the critical surface. In order to study the dynamics of the laser-plasma interaction, temporal information is also required. Because of the Fourier transform relationship ($\Delta\nu\Delta\tau \sim 0.5$), a streak camera coupled to a spectrometer cannot simultaneously provide both the required temporal and spectral resolution. Thus, a synchronized probe beam [3] was used instead, allowing the expansion to be measured with 250-fs time resolution [9].

Before discussing the experiment, we now derive approximate conditions under which the ponderomotive force becomes important. The dynamics of the laser-plasma interaction may be described mathematically by the two-fluid conservation equations of mass density, momentum, and energy. A one-dimensional treatment is sufficient since the gradients in the transverse direction (determined by the laser focal spot size) are much less than those in the parallel direction (determined by the density scale length). These equations are coupled to a collisional radiative model for the ionization stages, a modified Spitzer-Harm model for heat conductivity, and the Helmholtz wave equation for the electric field [10]. The momentum equation describing the motion of the ions to first order is given by [7]

$$\rho\partial v/\partial t + \rho(v\cdot\nabla)v \;=\; -\nabla P_e - n_e\nabla p_l \qquad (1)$$

The ion mass density is $\rho = n_i M$, the ion flow velocity is v, and the thermal pressure

equals the kinetic energy density, $P_e = n_e kT_e$, where kT_e is the electron temperature. The laser pressure on a single electron is the time-averaged quiver energy, $p_l = (1/2)m\langle v_{\rm os}^2\rangle$, which, by using $v_{\rm os} = eE/m\omega$, may be written as $p_l = (1/16\pi)(1/n_c)E^2$, where E is the electric field of the laser in the plasma, and n_c is the critical density.

Equation 1 may be solved analytically for the free isothermal expansion of the plasma into the vacuum—neglecting for the moment the last term, the ponderomotive force—yielding a density profile given by $n_e = n_0 e^{-z/d}$, where $d \equiv |n_e(\partial n_e/\partial z)^{-1}| = v_s \Delta t$ is the density scale length, and $v_s = (ZkT_e/M)^{1/2}$ is the acoustic velocity [7]. The expansion velocity of z_c is related to v_s, and hence the temperature, by $v_{\rm exp} = v_s \ln(n_0/n_c)$ (If a free adiabatic expansion is assumed, the relationship becomes $v_{\rm exp} = [2/(\gamma-1)]v_s$, where γ, the ratio of the specific heats, is chosen to be 1.7 [6]). The amplitude of the laser electric field E is determined by solving the Helmholtz equation, which for normal incidence is given by [7],

$$\frac{\partial^2 E}{\partial z^2} + \frac{\omega^2}{c^2}\epsilon(\omega, z)E = 0, \tag{2}$$

where $\epsilon = 1 - \omega_p^2/\omega(\omega + i\nu_{\rm ei})$ is the complex index of refraction of the plasma, $\nu_{\rm ei} \propto \ln\Lambda\ n_e Z/{kT_e}^{3/2}$ is the electron-ion collision frequency, Z is the average ionization state, and $\ln\Lambda$ is the Coulomb logarithm.

Figure 1 shows an exponential density profile, $n_e = n_0 e^{-z/d}$, calculated assuming the simple free expansion model discussed above. Here, n_0 is equal to a few (three) times solid density, and $d = 400$ Å, determined by using $ZkT_e \sim 2000$ eV in v_s and $\Delta t = 0.5$ ps, corresponding to the peak of a 1-ps pulse. Also shown is the square of the amplitude of the

electric field (E^2) calculated from Eq. 2. Near z_c, it also has approximately an exponential dependence on distance, $E^2(z) \propto e^{-z/l}$. Both quantities are normalized to unity. Figure 1 also shows that $l/d \sim 1$, *i.e.,* the scale length of $p_l \propto E^2$ is approximately equal to the scale length of $P_e \propto n_e$. Thus, since their scale lengths are comparable, only the ratio of the pressures matters in determining when the ponderomotive force $n_e \nabla p_l$ equals the thermal force ∇P_e at z_c. This condition is equivalent to the quiver energy of the electrons equalling their thermal energy, or,

$$m\langle v_{\rm os}^2 \rangle / 2kT_e \equiv 3.2 \times 10^{-13} I_{\rm inc} \lambda_0^2 / kT_e \sim 1 \tag{3}$$

($I_{\rm inc}$ is in W/cm^2, λ_0 is in μm, and kT_e is in eV). The electric field, and thus the quiver velocity, in the plasma were related to the incident light intensity, $I_{\rm inc}$, in Eq. 3 both by the fact that as the light wave approaches z_c, the peak value of E^2 is swelled by a factor of about 3.6 (shown in the numerical solution) over its vacuum value [7], $E_{\rm inc}^2$, and by the relationship $I_{\rm inc} \equiv (c/8\pi) E_{\rm inc}^2$.

We now discuss the experimental configuration. Laser pulses of wavelength 1.05 μm were generated in a Nd:glass laser system, which employed the technique of chirped pulse amplification [11] in order to keep the intensity in the amplifiers below the damage threshold of the glass. Two sets of experiments were performed: (1) a self-reflected Doppler shift measurement with 1-ps pulses; and (2) a pump-probe Doppler shift measurement using 400-fs pulses obtained after the laser system was upgraded to include a titanium:sapphire regenerative amplifier [12]. Using a third-order autocorrelator, the

intensity peak-to-background contrast ratio of the laser pulses was measured to be 10^3:1 for the 1-ps case, and $5 \times 10^5 : 1$ for the 400-fs case. For either case, the contrast ratio was further approximately squared by frequency-doubling ($\lambda = 0.53$ μm) the laser pulses using a KDP crystal. The maximum energy of the 0.53 μm pulse was about 80 mJ ($I_{\max} = 1.6 \times 10^{16}$ W/cm^2 for 400-fs pulses and $I_{\max} = 6 \times 10^{15}$ W/cm^2 for 1-ps pulses). The laser was then focused at normal incidence ($\theta = 0°$) in a vacuum chamber onto various solid targets, which were rastered between shots. The focused spot size was measured at full power in vacuum with a 20$\times$ magnifying imaging system and a digital charge-coupled device (CCD) camera. With this peak intensity and contrast ratio, the intensity of light prior to the main pulse was well below the ionization threshold of the target.

We first discuss the results obtained from the spectra of the self-reflected 1-ps pump incident on aluminum. Here the spectra of the incident and reflected light were recorded separately with a spectrometer. A Doppler shift to the blue and a broadening — characteristic of an expanding plasma [6] — were observed and are shown in Fig. 2 (b) for an intensity $I_{\rm inc} \sim 2 \times 10^{15}$ W/cm^2. The measured Doppler shift agrees quite well with a Doppler shift predicted by the simulation with the laser parameters used in the experiment and ponderomotive force included, as shown in Fig. 2 (c), given the measured incident light spectrum shown in Fig. 2 (a). That the free expansion model is inadequate is dramatically demonstrated in Fig. 2 (d), which shows the Doppler shift calculated in the simulation without including the ponderomotive force in Eq. 1; it is three times greater than the

measured shift (Figs. 2 (b)). This translates into a difference in ZkT_e of a factor of approximately ten. Conversely, if the measured $\Delta\lambda/\lambda$ were used to estimate ZkT_e using the simple analytical model that assumes either isothermal, or adiabatic, free expansion, an underestimate ($ZkT_e < 150$ eV) by the same amount would be obtained. This disagreement comes as no surprise, since from Eq. 3, using our laser parameters and the temperature obtained from the simulation, $kT_e \sim 200$ eV, we would expect the free expansion model to be inaccurate.

Further evidence that the laser pressure balances the thermal pressure is found in the observed constancy of the Doppler shift with variation of the laser intensity. As the laser intensity was increased—by increasing the laser energy, keeping the pulse width constant—from $I_{\rm inc} \simeq 5 \times 10^{14}$ W/cm^2 to $I_{\rm inc} \simeq 2 \times 10^{15}$ W/cm^2, a factor of four, the Doppler shift was observed to remain constant within the experimental uncertainty, $\simeq$ 10%. However, a bandpass-filtered soft x-ray diode array indicated that the temperature increased over the same range of laser energy. Neglecting the fact that the absorption may change slightly with intensity over this range, it is expected that a linear increase in intensity, and thus absorbed laser energy, should result in roughly a linear increase in temperature. Thus, if the ponderomotive pressure played no role, the resulting linear increase in thermal pressure should have resulted in an increase in the Doppler shift by at least the square root of this change, or a factor of two. In fact, an even greater increase is expected because of the expected increase of Z with T_e. The fact that this was not

observed is consistent with the interpretation that the increase in thermal pressure was compensated by a corresponding increase in ponderomotive pressure, a trend which was also confirmed in the simulation.

We now discuss a pump-probe experiment using 400-fs pulses incident on a molybdenum target [13]. In this case a two-dimensional CCD was used as the multichannel analyzer with the spectrometer, so that the spectra of the incident and specularly reflected probe beam could be simultaneously recorded by focusing the two beams to different locations along the spectrometer's entrance slit. The target was also rastered between shots. The 0.5-μm probe pulse, beam-split from the pump, with final intensity less by a factor of 10^{-4}, was incident at 25° to the target normal. It may be seen from the relation $n = n_c \cos^2\theta$ that the probe will be reflected at $0.8n_c$. Given the steep density gradient, this is very close to the pump's critical surface (≤ 60 Å). In order to assure that the probe only sampled the hot central region of the plasma that was created by the pump, it was focused with a faster lens to a focal spot that was only about one half of the pump's. The centers of their focal spots were aligned to within 20% of the pump's focal spot with a 5×-magnification imaging lens and displayed on a digitizing CCD camera. Additionally, only about the central 10% of the reflected probe beam was sampled by the spectrometer by the use of an aperture. The delay between the pump and probe could be varied to within an accuracy of about 100 fs. Spectra were recorded as the time delay was varied. The time when they overlapped, $t = 0$, was determined to within approximately half a

pulse width ($\sim$ 200-fs) accuracy by observing interference fringes formed by beating the probe and scattered pump light. For this purpose the laser operated in the 10 Hz alignment mode (much weaker intensity), and the target was not moved between shots. Thus the scattered pump light intensity from the already-damaged spot was on the same order of magnitude as the probe beam in the latter's specular reflection direction.

Figure 3 shows $\Delta\lambda$ as a function of delay at pump laser intensity $I \sim 10^{16}$ W/cm^2. For clarity, the Gaussian temporal profile of the pump laser is also shown on a normalized linear scale. Five shots were fired at each time delay, and Fig. 3 shows the average of spectral-intensity weighted shift of these shots:

$$\Delta\lambda = \left[\frac{\int \lambda I(\lambda) d\lambda}{\int I(\lambda) d\lambda}\right]_{\text{reflected}} - \left[\frac{\int \lambda I(\lambda) d\lambda}{\int I(\lambda) d\lambda}\right]_{\text{incident}}.$$

Beginning with negative delay times, corresponding to the probe preceding the pump, as the delay time in Fig. 3 is increased, or as the delay between the pump and probe is decreased, the Doppler shift is observed to increase. This is attributed to an expected increase in the plasma temperature as the pump laser intensity increases. Evidence of a Doppler shift several pulse widths (2 ps) before the peak of the pump may be explained by the fact that a plasma is produced at an intensitiy that is several orders of magnitude ($\sim$ 4) below the pump's peak intensity, and the foot of the pulse at this intensity is 2 ps before the peak. A local minimum is observed in the Doppler shift centered near $t = 0$, when the pump and probe beam overlap in time. This is consistent with the expected effect of the ponderomotive force, which also maximizes at $t = 0$, when the pump intensity

maximizes. Finally, when the probe follows the pump by a time equal to approximately a pulse width, the shift begins to decrease. This is expected since after the peak of the pump intensity, plasma heating decreases and both expansion and diffusion lead to rapid cooling. At later times, v_{exp} reaches a plateau within the limits of the uncertainty given by the error bars in Fig. 3, and even increases slightly. This indicates that the cooling rate decreases, possibly becoming less than the heating rate. This is also expected since the thermal pressure gradient, which drives the expansion and thus the cooling, decreases with time as the plasma expands.

In conclusion, the ponderomotive force will affect those processes that depend strongly on the evolution of the density profile if the conditions given by Eq. 3 are met. Specifically, the simple relation between the Doppler shift of the reflected pump laser light and the electron temperature, as given by the free expansion model, does not apply in this case. Resonance absorption of the laser light — because it depends strongly on the density scale length near the critical surface — and expansion cooling of the plasma are important processes that are affected. Finally, an intriguing implication of this study is that at higher intensities, the ponderomotive force of an intense short pulse laser might be used to significantly compress and thus ignite a laser-fusion target.

This work was partially funded by the National Science Foundation Center for Ultrafast Optical Science, contract #PHY8920108. The authors would like to thank N. Schryer for the computer algorithm used in the numerical simulations and G. Mourou for

many encouraging discussions.

References

[1] M.M. Murnane, H.C. Kapteyn, and R. W. Falcone, *Phys. Rev. Lett.* **62**, 155 (1989).

[2] J.C. Kieffer, P. Audebert, M. Chaker, J.P. Matte, H. Pepin, T.W. Johnston, P. Maine, D. Meyrhofer, J. Delettrex, D. Strickland, P. Bado, G. Mourou, *Phys. Rev. Lett.* **62**, 760 (1989).

[3] O. L. Landen, D. G. Stearns, and E. M. Campbell, Phys. Rev. Lett. **63**, 1475 (1989).

[4] R. L. Fedosejevs, R. L. V. Tomov, N. H. Burnett, G. D. Enright, and M. C. Richardson, Phys. Rev. Lett. **39**, 932 (1977); D. T. Attwood, D. W. Sweeney, J. M. Auerbach, and P. H. Y. Lee, Phys. Rev. Lett. **40**, 184 (1978); W. B. Fechner, C. L. Shepard, Gar. E. Busch, R. J. Schroeder, and J. A. Tarvin, Phys. Fluids **27**, 1552 (1984).

[5] R. E. Kidder, "Interaction of Intense Photon Beams with Plasmas," in *Proceedings of the Japan-U.S. Seminar on Laser Interaction with Matter*, C. Yamanaka, ed. (Tokyo International Book, Tokyo, 1973); K. Lee, D. W. Forslund, J. M. Kindel and E. L. Lindman, Phys. Fluids, **20**, 51 (1977).

[6] H. M. Milchberg, R. R. Freeman, and S. C. Davey, Phys. Rev. Lett. **61**, 2364 (1988); H. M. Milchberg, and R. R. Freeman, Physical Review A **41**, 2211 (1990).

[7] W. L. Kruer, *The Physics of Laser Plasma Interactions* (Addison-Wesley, New York, 1988), 116.

[8] The resonant excitation of electrostatic plasma waves at z_c will also result in density profile modification (*ibid.*).

[9] When a probe beam was used, θ in the above equation for the Doppler shift became the angle of incidence of the probe beam.

[10] D. Umstadter, H. Milchberg, T. McIlrath and R. R. Freeman, "The Dynamics of Dense Plasmas Produced by Ultra-Short Pulse Lasers", in *Digest of Topical Meeting on High Energy Density Physics with Subpicosecond Laser Pulses, 1989* (Optical Society of America, Washington, D.C., 1989).

[11] P. Maine, D. Strickland, P. Bado, M. Pessot and G. Mourou, IEEE J. Quantum Electron. **QE-24**, 398 (1988).

[12] G. Mourou and D. Umstadter, "The Development and Applications of Compact High-Intensity Lasers", to appear in Phys. Fluids (1992).

[13] An aluminum target was also used in the pump-probe experiment. However, it was found that the Al target scattered much more pump light into the probe's specular

reflection direction—up to 30% – 50% of the probe, compared to $\leq$ 10% for the Mo target. The scattered pump light entered the spectrometer and interfered with the probe light. This made the interpretation of the Al data more difficult.

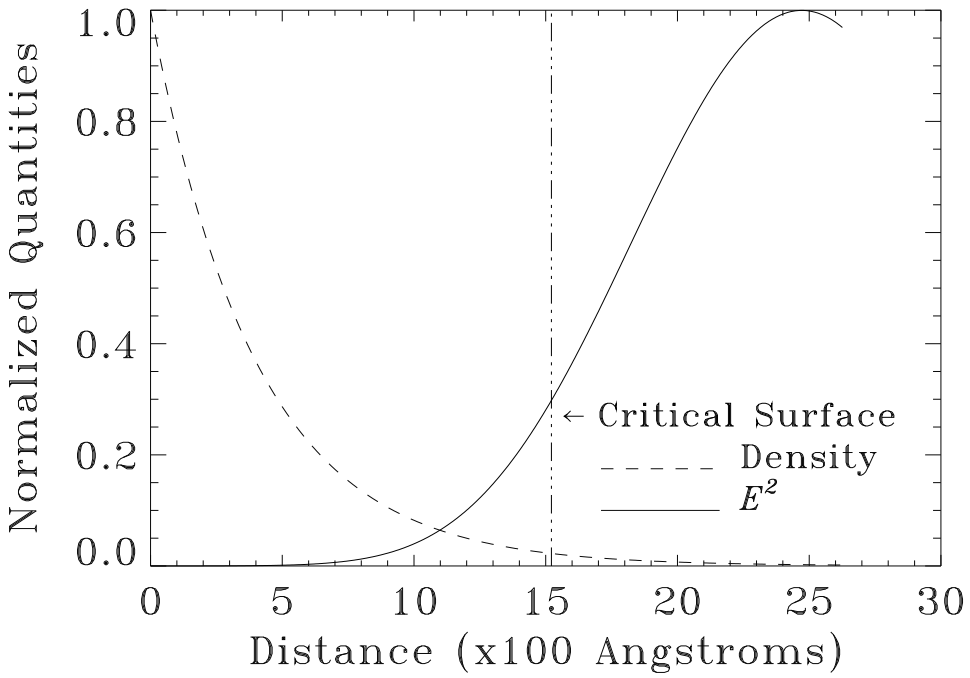

Figure 1: An exponential density profile, $n_e = n_0 e^{-z/d}$, calculated assuming the simple free expansion model. Here, n_0 is equal to a few (3) times solid density, and $d = 400$ Å, determined by using $ZkT_e \sim 2000$ eV in v_s and $\Delta t = 0.5$ ps, corresponding to the peak of a 1-ps pulse. Also shown is the square of the amplitude of the electric field (E^2) calculated from Eq. 2. Near z_c, it also has an exponential dependence on distance, $E^2(z) \propto e^{-z/l}$. Both quantities are normalized to unity. The fact that the ratio of their scale lengths is approximately unity ($d/l \sim 1$) indicates that only the ratio of the pressures (Eq. 3) matters in determining when the ponderomotive force is comparable to the thermal expansion force.

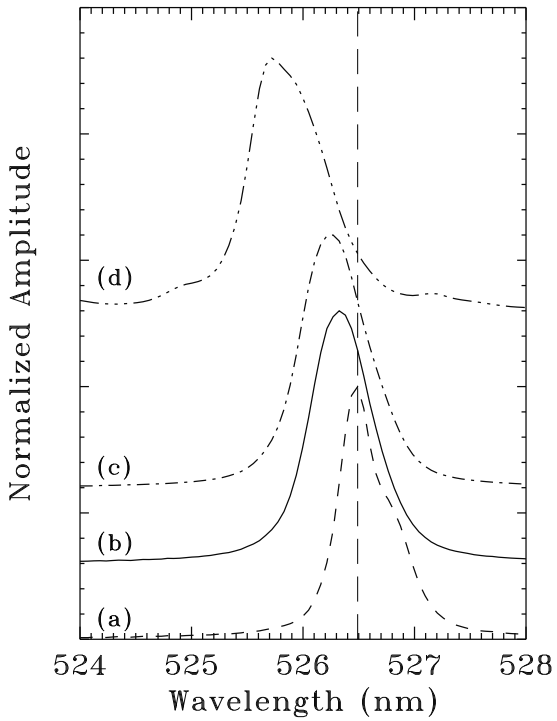

Figure 2: Spectrum of pump light: (a) incident on the target; (b) reflected from the moving critical surface, measured experimentally, $I \simeq 2 \times 10^{15}$ W/cm^2; (c) calculated numerically with the ponderomotive force included; and (d) calculated numerically without the ponderomotive force. If the measured $\Delta\lambda/\lambda$ from (b) were used to estimate ZkT_e using the simple analytical model that assumes either isothermal, or adiabatic, free expansion, an underestimate of v_{exp} by by a factor of three, and ZkT_e, by a factor of ten would be obtained.

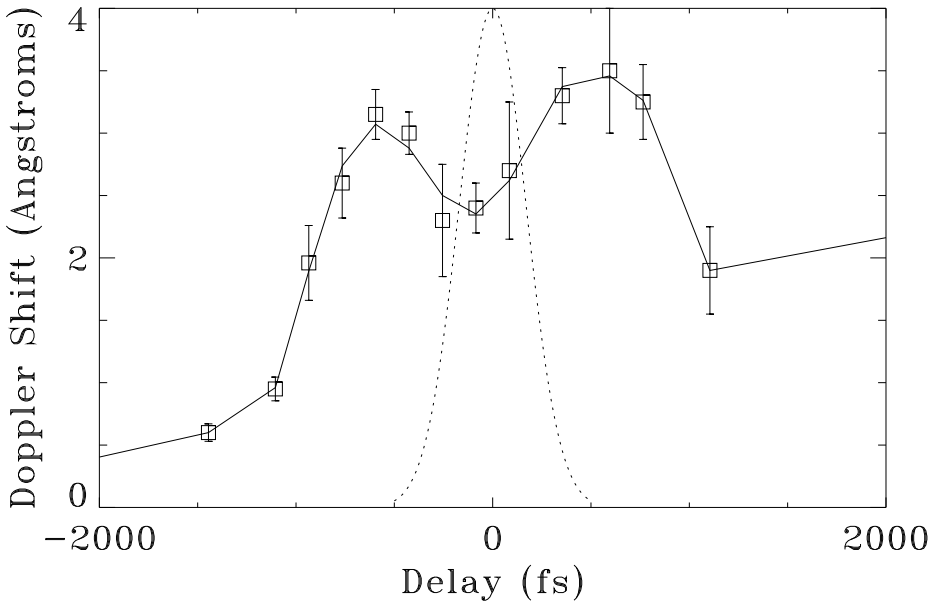

Figure 3: The Doppler shift of the reflected probe beam, due to motion of the critical surface [$n_c(\text{probe}) = 0.8 n_c(\text{pump})$], as a function of delay between the pump and probe (solid line). A dip at $t = 0$ indicates that the ponderomotive force impedes the thermal expansion of the plasma. The normalized Gaussian temporal profile of the laser is superimposed for clarity (dotted line).